Arch. Metall. Mater. **64** (2019), 2, 759-764

DOI: 10.24425/amm.2019.127610

R. BOGUCKI*#, M. BASIAGA, A. ŻYRA**#

THE EVALUATION OF RESISTANCE TO CRACKING OF Ti10V2Fe3Al ALLOY CHARACTERIZED BY DIFFERENT MORPHOLOGY AND VOLUME FRACTION OF α-PHASE PRECIPITATES

The paper presents the results of the Ti10V2Fe3Al alloy crack resistance assessment using the Rice's J-integral technique as a function of morphology and volume fraction of α-phase precipitates. Titanium alloys characterized by the two-phase structure $\alpha + \beta$ are an interesting alternative to classic steels with high mechanical properties. Despite the high manufacturing costs and processing of titanium alloys, they are used in heavily loaded constructions in the aerospace industry due to its high strength to density ratio. The literature lacks detailed data on the influence of microstructure and, in particular, the morphology of α phase precipitates on fracture toughness in high strength titanium alloys. In the following work an attempt was made to determine the correlation between the microstructure and resistance to cracking in the Ti10V2Fe3Al alloy.

Keywords: fracture mechanical, Rice's J-integral, stress induced martensite (SIM), metastable β titanium alloy

1. Introduction

Titanium alloys are characterized by high mechanical and good fracture toughness, comparable to high strength alloy steels at a much lower specific gravity. They are used in the aircraft and aerospace industries due to their high specific strength. The microstructure and mechanical properties of titanium alloys are strongly related to its chemical composition. High mechanical properties are obtained in titanium alloys with a β and $(\alpha + \beta)$ microstructure, which are stabilized by alloying additives such as V, Fe, Nb [1-4]. Ti10V2Fe3Al is a metastable β-alloy. In this alloy, the shape and volume fraction of α-phase precipitates can be controlled by the temperature and time of heating [5-7]. It has been observed that with the participation of the α phase, below 50% the phenomenon of stress-induced martensite (SIM) [5-6, 8-9] is revealed.

Titanium alloys designed for aircraft constructions should have high resistance to cracking. A particularly dangerous phenomenon is the formation of low and high cycle fatigue cracks. This problem has been well described in the literature [10-14]. Another extremely important aspect is the quantitative estimation of fracture toughness. This problem is dealt with by fracture mechanics [15]. This problem is widely described for the classic Ti6Al4V alloy [16-18]. In the case of the Ti10V2Fe3Al alloy, there are few papers on the fracture toughness assessment using classical fracture mechanics [19-21].

For the basic techniques to assess fracture toughness, we include the stress intensity factor K_{Ic} determined in a plane strain, Rice's J-integral J_{Ic} and the critical value of the crack-tip opening displacement CTOD. For materials with relatively high toughness, the best approach to assessing crack resistance is to use the Rice's J-integral. In the presented work, the Rice's J-integral method was adopted as the criterion for assessing fracture toughness as determined by the susceptibility technique in accordance with ASTM E-399.

2. Experimental procedure

The Ti10V2Fe3Al alloy provided in the form of a forging was used for the tests. The chemical composition is shown in Table 1. The beta transformation temperature was 828°C [5]. The heat treatment of the alloy was carried out in a Nabertherm P330 tubular furnace under an argon shield. Two heat treatment schemes were used. The first diagram ($\beta + (\alpha + \beta)$) consisted of pre-heating to 900 °C at a speed of 10 K/min and annealing for 20 minutes. The samples were then cooled with the furnace at a speed of 10 K/min to 700°C and annealing for 15 and 60 minutes followed by cooling in water. The second scheme ($\alpha + \beta$) consisted of heating at a speed of 10 K/min to a temperature

TABLE 1

Chemical composition of Ti10V2Fe3Al alloy

Material	V	Al	Fe	O	N	C	Ti
Ti10V2Fe3Al	9.9	2.9	1.9	0.13	0.007	0.002	Bal.

* CRACOW UNIVERSITY OF TECHNOLOGY, DEPARTMENT OF MECHANICAL ENGINEERING, INSTITUTE OF MATERIALS SCIENCE, 37 JANA PAWŁA II AV, 31-864 KRAKÓW, POLAND
** CRACOW UNIVERSITY OF TECHNOLOGY, DEPARTMENT OF MECHANICAL ENGINEERING, INSTITUTE OF PRODUCTION ENGINEERING, 37 JANA PAWŁA II AV, 31-864 KRAKÓW, POLAND
# Corresponding authors: rbogucki@mech.pk.edu.pl, agazyra@gmail.com

of 700°C and annealing for 5 min, the next sample was heated to 775°C with annealing for 120 min with subsequent cooling in water. The samples prepared in this way were subjected to microscopic tests, stereological analysis, mechanical properties, fracture toughness and fractography observations.

Observations of the microstructure were performed using scanning electron microscope JOEL JSM5510LV. Metallographic samples were polished with 6 and 1 μm diamond pastes and then chemically etched in a solution of 10 ml HNO_3 + 20 ml HF + 20 ml glycerine. The volume fraction of the α-phase was determined using Image J software with a total analysis field of 1 mm^2. Hardness measurements were carried out using the Vickers method at 30 kg load, performing 10 indents and determining the average. A static tensile test was carried out on a MTS Criterion Model 43 testing machine at ambient temperature. Cylindrical samples with a diameter of 5 mm and a measuring length of 25 mm were used for the tests. To assess the cracking resistance using the Rice's J-integral method, a susceptibility method was used to determine J_{Ic} using one sample. The test was carried out on 12 mm wide compact samples with a previously performed fatigue crack. The procedure was carried out according to ASTM E-399. In order to control the development of pre-cracking, the surfaces of the samples were polished. The pre-cracking process was performed on an Instron 8511.20 pulsation testing machine using a pulse load of 100 Hz. The MTS Criterion Model 43 testing machine was used for the tests. The development of fatigue cracks and breakthroughs was performed on the scanning electron microscope JOEL JSM5510LV.

3. Results

3.1. Microstructure

The purpose of the heat treatment was to create a microstructure with different morphology and volume fraction of the α phase in the analysed titanium alloy, table 2. The material was delivered in the form of forgings with deformed bimodal structure [5]. The first scheme led to recrystallization of the deformed β phase grains. Annealing above the β-transformation caused dissolution of the alpha phases. Subsequent cooling below the β-transition led to the initiation of α phase precipitation from the supersaturated β solid solution that formed the acicular precipitates, Fig. 1a and b. After annealing at 700°C for 15 minutes, the volume fraction of α phase at the level of 9.1%, was obtained Fig. 1a. Extending the soaking time to 60 min led to an increase of alpha phase volume fraction to 62.1%, Fig. 1b. The use of the second scheme, where the soaking process was carried out below the β-transformation temperature, resulted in a different morphology of the precipitates. Annealing at 700°C for 5 min led to obtaining globular precipitations of the α phase with a volume fraction of 62.1%. The results shows that extending the time of annealing doesn't change the volume fraction of α phase but leads to a change in the shape of precipitates from globular to elongated [5,6]. In order to reduce the volume fraction of α phase, the heating temperature was increased to 775°C and the soaking time to 120 min. This allowed obtaining globular precipitations of the α phase with a volume fraction of 15.4%.

TABLE 2

The volume fraction of phase as a function of heat treatment

	Heat treatment	Morphology and volume fraction of α phase
1	900°C+700°C/ 15 min.	acicular: 9.1%
2	900°C+700°C/ 60 min.	acicular: 62.1%
3	775°C/ 120 min.	globular: 15.4%
4	700°C/ 5 min.	globular: 58.5%

3.2. Mechanical properties

The mechanical properties results are summarized in Table 3. Hardness measurements didn't reveal any significant differences in the analysed structures. The highest hardness of 292 HV was observed for the sample after annealing in accordance with scheme II ($\alpha + \beta$) at 700°C for 5 min. The lowest hardness level of 273 HV was obtained in scheme II ($\alpha + \beta$) after annealing at 775°C for 120 min. The analysis of stretching curves revealed the occurrence of the phenomenon of martensitic transformation induced by plastic deformation, Fig. 2 and 3. The SIM was observed after annealing at 1 and 2 heat treatment. The highest mechanical properties were observed in the case of the sample annealing at 700°C for 5 min. The yield strength (YS) was 845 MPa, tensile strength (UTS) 899 MPa at an extension of 15.9%.

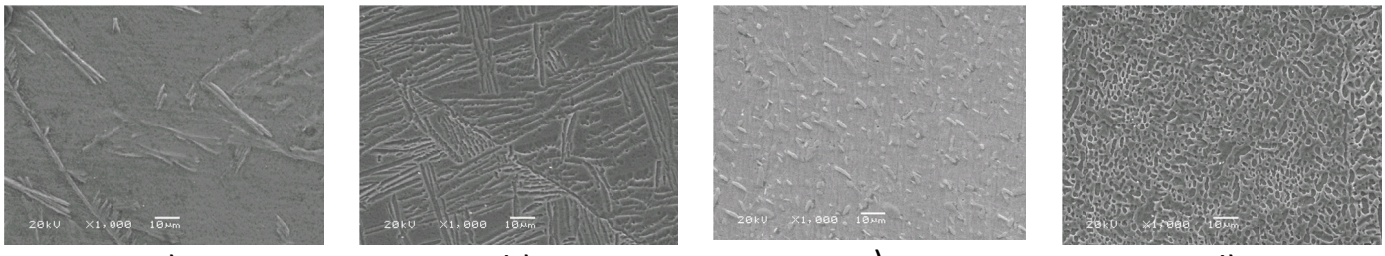

Fig. 1. SEM micrographs of specimen with different heat treatment: a) acicular α phase in β matrix (900°C+700°C/15 min), b) acicular α phase in β matrix (900°C+700°C/60 min), c) globular α phase in β matrix (775°C/120 min), d) globular α phase in β matrix (700°C/5 min)

TABLE 3

Mechanical properties of titanium Ti-10V-2Fe-3Al alloy after different heat treatments

Heat treatment		$YS_{0,2}/YS_{0,2SIM}$ [MPa]	UTS, [MPa]	Elongation [%]	Hardness	
					HV30	Standard deviation
1	900°C+700°C/15 min	454	880	19.0	288	6.05
		790*				
2	900°C+700°C/60 min	772	820	12.2	289	6.61
3	775°C/ 120 min	563	881	17.8	273	4.03
		813*				
4	700°C/ 5 min	845	899	15.9	292	7.12

* – the second yield strength.

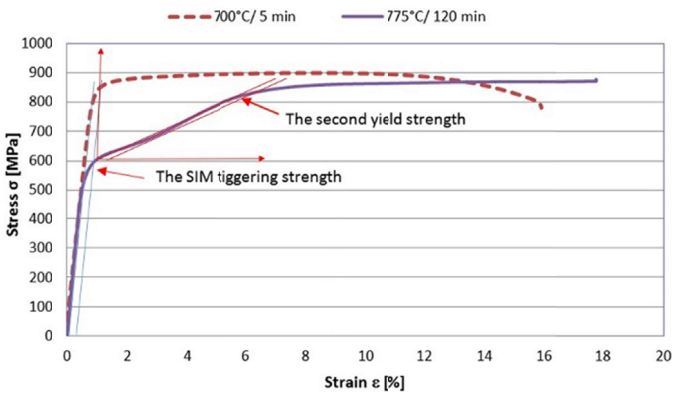

Fig. 2. Stress-strain curves for samples with globular alpha phase as a function of heat treatment. The graph shows the method of determining SIM triggering stress and the second yield stress

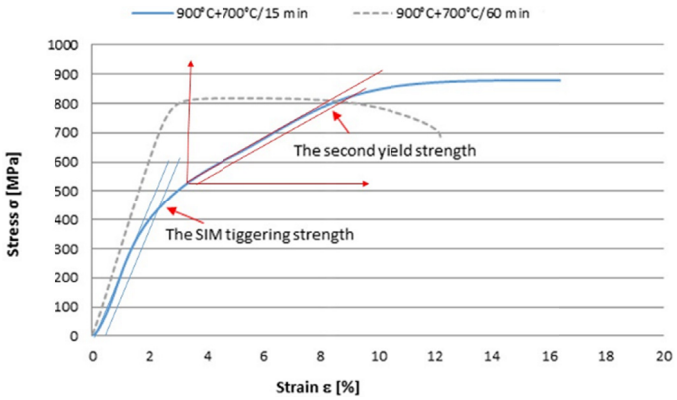

Fig. 3. Stress-strain curves for samples with acicular alpha phase as a function of heat treatment. The graph shows the method of determining SIM triggering stress and the second yield stress

The lowest strength and elongation was obtained in the 2 heat treatment. The YS was 772 MPa, UTS 820 MPa and elongation 12.2%. The highest elongation was obtained in the 900°C+700°C scheme after annealing for 15 min and amounted to 9.1%.

3.3. Mechanical fracture

The Rice integral criterion using the susceptibility method was used to assess fracture toughness. The analysis of the development of fatigue cracks revealed that in the case of particles of the α phase in a globular form, it runs between the particles, Fig. 4c and d. A different mechanism was observed for the acicular particles. The process of fatigue cracking proceeded between particles as well as particles. At the same time, there was a tendency to change the direction of crack growth after crossing the barrier, in the form of acicular particles, Fig. 4a and b.

The susceptibility method used to determine fracture toughness is based on cyclic unloaded compact samples. In this way, a characteristic course of the graph is obtained as shown in Fig. 5. On the basis of the value of energy absorbed by the sample, the value of potential energy change in the fracture area was determined, whereas the value of the crack growth was determined on the basis of the change in the angle of inclination of subsequent strains. As a result, a graphical dependence of the potential energy change J in the crack growth function Da was obtained, as shown in Figure 6.

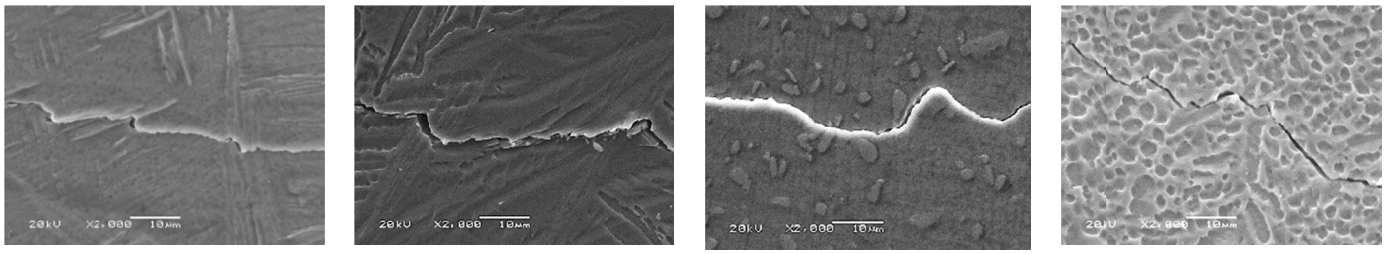

Fig. 4. Propagation of fatigue cracks in the microstructure after heat treatment: a) 900°C+700°C/15 min, b) 900°C+700°C/60 min, c) 775°C/ 120 min, d) 700°C/ 5 min.

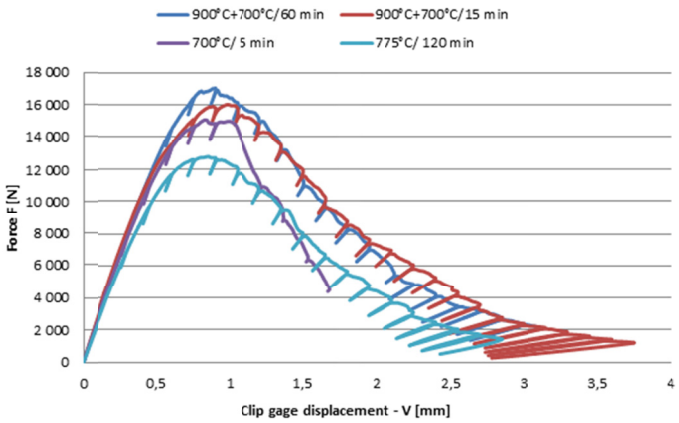

Fig. 5. Diagram of force dependence as a function of crack opening for tested samples

The value of the critical J-integral of Rice's (J_{Ic}), was defined as the point of intersection of the curve R with the blunt line shifted to the value of 0.2 mm, Fig. 6. On the basis of the defined critical value of the J_{Ic}, the critical plane strain fracture toughness K_{ic} was determined, table 4. The results obtained are summarized in Table 4. It was observed that the highest cracking resistance was found in the sample after annealing in accordance with 2 heat treatment and it was J_{Ic} = 156 kJ/m^2 and K_{ic} = 114 MPa m$^{-1/2}$. The lowest crack resistance was characterized by the sample after annealing at 775 °C for 120 min. The fracture toughness values were 55 kJ/m^2 and 82 MPa m$^{-1/2}$, respectively.

Fractographic observations of samples after Rice's integral revealed that in all analysed fractures, characteristic microvoids are visible, showing that the cracking was ductile, Fig. 7.

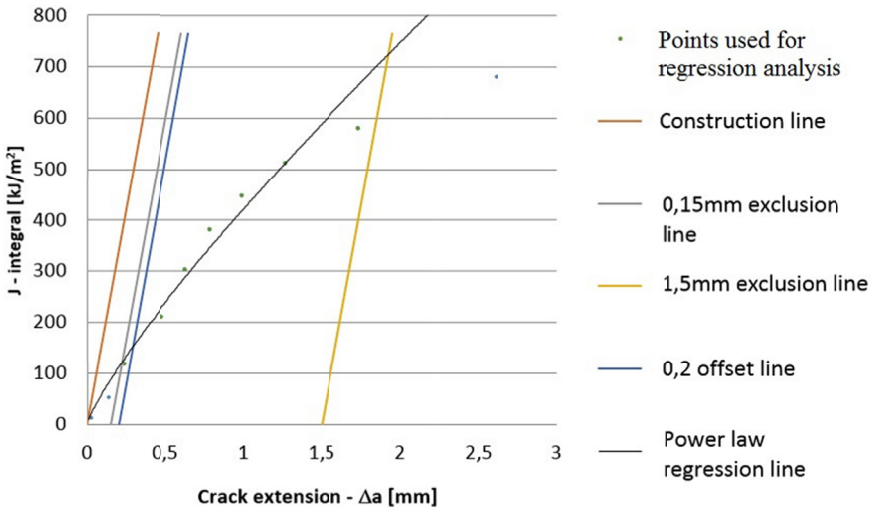

Fig. 6. The determination of the critical value J_{Ic} for the heat treatment 900°+700°C 60 min.

TABLE 4

Results of resistance to cracking as a function of heat treatment

	Heat treatment	Critical J-integral of Rice's – J_{Ic} kJ/m^2	Critical plane strain fracture toughness – K_{Ic} MPa m$^{-1/2}$	Volume fraction of α phase [%]
1	900°C+700°C/15 min.	97	96	9.1
2	900°C+700°C/60 min.	156	114	62.1
3	775°C/120 min.	55	82	15.4
4	700°C/ 5 min.	122	100	58.5

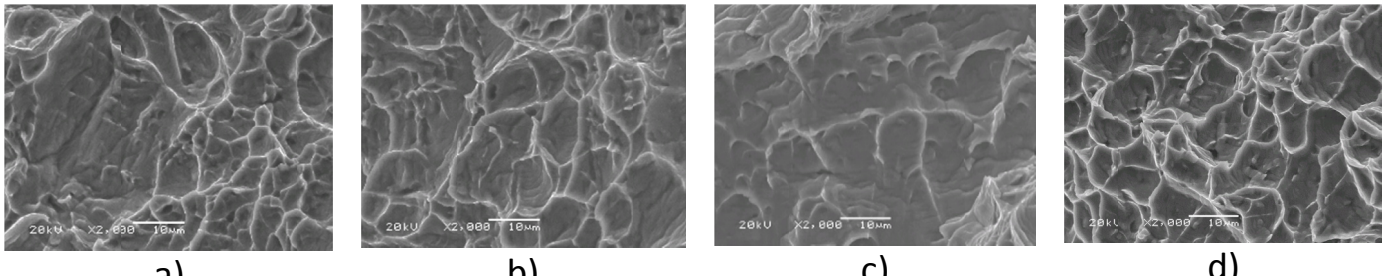

Fig. 7. Topography of fractures of samples after the study of Rice's integral: a) 900°C+700°C/15 min, b) 900°C+700°C/60 min, c) 775°C/120 min, d) 700°C/5 min.

4. Discussion

The applied heat treatment made it possible to obtain different morphology and volume fraction of α phase in Ti10V2Fe3Al alloy. The increase in the volume fraction of alpha phase led to an increase in hardness. With the participation of the alpha phase below 16%, the occurrence of martensitic transformation induced by plastic strain was observed, Fig. 2 and 3, which was confirmed in the works [2,5-6].

The SIM phenomenon slightly improves the durability, measured during the tensile test. The best combinations of mechanical properties were obtained in scheme II after annealing at 700°C for 5 min. With the volume fraction of the globular α phase 58.5%, yield strengths were found at 845 MPa and UTS at 899 MPa, with an elongation of 15.9%.

It was observed that higher mechanical properties were obtained in samples with globular α phase particles. The reason for this is probably the morphology of α particles that have a regular globular shape and are evenly distributed in the matrix. The lower strength in 1 and 2 heat treatment should be explained by the presence of the α phase in the form of acicular. Probably during plastic deformation, the needle-like α precipitates cracks brittle which may cause nucleation of microcracks that weaken the material.

The increase in ductility of the material is one of the ways to improve fracture toughness. Phenomena such as phase transformation, occurrence of the second phase in the matrix may also contribute to the improvement of fracture toughness. In the analysed alloy it was observed that the crack resistance measured by Rice J-integral is the highest for the sample characterized by the highest volume fraction of the acicular α phase. The value 156 kJ/m^2 was obtained after annealing according to 2 heat treatment where the volume of acicular phase was 62.1%. The lowest crack resistance of 55 kJ/m^2 was recorded in the structure characterized by globular precipitation of the α phase and the volume of 15.4%.

The lower resistance to cracking of samples with the phenomenon of SIM was interesting. It was assumed that martensitic transformation induced by plastic deformation, occurring on the forehead of the fracture, will constitute an additional energy contribution leading to an increase in resistance to cracking. In TRIP (Transformation-Induced Plasticity) steel, martensitic transformation induced by plastic deformation, occurring before breakage, is associated with local increase of compressive stresses which inhibits crack propagation [22]. In titanium alloys, martensitic transformation is an ineffective mechanism of strengthening compared to steel, hence probably its low impact on the crack inhibition process in the tested Ti10V2Fe3Al alloy.

Higher resistance to cracking of the microstructure with a high proportion of particles α phase can be explained by blocking the propagation of the crack by acicular precipitates. This mechanism is based on a change in the direction of crack propagation, which in turn leads to an increase in cracking energy. This phenomenon was observed in the case of the development of fatigue cracks, Fig. 4a and b, where a change in the direction of crack propagation at the matrix-needle interface of the α phase was observed. It seems to have a beneficial effect on the inhibition of crack propagation in the vicinity of sharp failure

An increase in the volume fraction of acicular alpha phase caused a decrease in ductility in a static tensile test. The decohesion process in this test is related to the nucleation of microvoids around the precipitates, their growth and coalescence. As observed in [7], the crack nucleation process in the tested titanium alloy depends on the orientation of secondary precipitates to the direction of the load. When the particles of the acicular alpha phase are orientated perpendicularly to the load direction, this leads to local concentration of stresses and acceleration of the nucleation and propagation of the crack.

High resistance to cracking in all analysed structures was confirmed by observations of the topography of fractures obtained after the Rice'a J-integral samples. The fractures of the observed samples were of a ductility nature. It was observed that samples with the highest Jic value showed features of greater plastic deformability. This is evidenced by stronger warp deformation in the areas of microvoids, Fig. 7b and d.

5. Conclusions

1. The applied heat treatment allowed to obtain different morphology and volume fraction of α phase in Ti10V2Fe3Al alloy.
2. The highest mechanical properties were obtained for the alloy with globular particles with a volume fraction of 58.5%.
3. The highest resistance to cracking was characterized by microstructure with acicular particles with a volume fraction of 62.1%.
4. There was no effect of the SIM transformation on the increase of resistance to cracking. The lowest resistance to cracking was found in samples with the lowest volume fraction of the α phase.

REFERENCES

[1] T.W. Duerig, J. Albrecht, D. Richer, P. Fischer, Acta Metall. **30**, 2161-2172 (1982)

[2] J. Kawałko, M. Wroński, M. Bieda, K. Sztwiertnia, K. Wierzbanowski, D. Wojtas, M. Łagoda, P. Ostachowski, W. Pachla, M. Kulczyk, Materials Characterization **141**, 19-31 (2018).

[3] R. Dąbrowski, Arch. Metal. Mater. **56**, 703-707 (2011)

[4] G. LüterIng, J.C. Williams, Titanium, second ed., Springer, Berlin 2007.

[5] R. Bogucki, K. Mosór, M. Nykiel, Arch. Metal. Mater. **59**, 1269-1273 (2014).

[6] C. Li, X. Wu, J.H. Chen, S. Vander Zwaag, Mater. Sci. Eng. **A 528**, 5854-5860 (2011).

[7] G.T. Terlinde, T.W. Duerig, J.C. Williams, Metallurgical Transactions A, **14A**, 2101-2115 (1983).

[8] A. Bhattacharjee, S. Bhargava, V.K. Varma, S.V. Kamat, A.K. Gogia, Scripta Materialia **53**, 195-200 (2005)

[9] Wei Chen, Qiaoyan Sun, Lin Xiao, Jun Sun, Materials Science and Engineering A **527**, 7225-7234 (2010).

[10] Ying Wua, Jianrong Liua, Hao Wanga, Shaoxuan Guana, Rui Yanga, Hongfu Xiang, Journal of Materials Science & Technology **34**, 1189-1195 (2018) .

[11] 0. Umezawa, K. Nagai, T. Yuri, T. Ogata, K. Ishikawa, Advances in Cryogenic Engineering Materials **38**, 175-182 (1992)

[12] S.Q. Zhang, S.J. Li, M.T. Jia, F. Prima, L.J. Chen, Y.L. Hao, R. Yang, Acta Materialia **59**, 4690-4699(2011).

[13] Y. Ono, T. Yuri, H. Sumiyoshi, S. Matsuoka, T. Ogata, Cryogenics **43**, 483-489 (2003).

[14] R.O. Ritchie, D.L. Davidson, B.L. Boyce, J.P. Campbell, O. Roder, Fatigue Fract. Eng. Mater. Struct. **22**, 621-631 (1999).

[15] R. Bogucki, Arch. Metal. Mater. **54**, 1073-1082 (2009).

[16] Xian-Kui Zhu, James A. Joyce, Engineering Fracture Mechanics **85**, 1-46 (2012).

[17] S.G. Ivanova, R.R. Biederman, R.D. Sisson Jr., Journal of Materials Engineering and Performance **11** (2), 226-231(2002).

[18] Zhang Junhong, Yang Shuo, Lin Jiewei, Chinese Journal of Mechanical Engineering **28** (2), 409-415 (2015).

[19] O. Quénard, O. Dorival, Ph. Guy, A. Votié, K. Brethome, Springer, published online: 03 April 2018.

[20] T.W. Duerig, J.E. Allison, J.C. Williams, Metallurgical Transactions A **16A**, 739-751(1985).

[21] R.R. Boyer, G.W. Kuhlman, Metallurgical Transactions A **18A**, 2095-2103 (1987).

[22] S.K. Jha, K.S. Ravichandran, Metallurgical and Materials Transactions A **31A**, 703-714 (2000).

[23] J. Kobayashi, D Ina, A Futamura, K. Sugimoto, ISIJ International **54**, 4, 955-962 (2014).